PROCEEDINGS OF SCIENCE

First Measurement of Differential Charged Current Quasielastic-like ν_μ-Argon Scattering Cross Sections with the MicroBooNE Detector

Afroditi Papadopoulou[a,*]

[a] *Massachusetts Institute Of Technology, 77 Massachusetts Avenue, Cambridge, MA, USA*

E-mail: apapadop@mit.edu

This poster reports on the first measurement of flux-integrated single differential cross sections for charged-current muon neutrino scattering on argon with a muon and a proton in the final state. The measurement was carried out using the MicroBooNE liquid argon time projection chamber detector and the Booster Neutrino Beam at Fermi National Accelerator Laboratory. An event selection is applied to enhance the contribution of charged-current quasielastic interactions. Our results are reported in the form of differential cross sections as a function of the final state muon and proton kinematics. The resulting differential cross sections illustrate an overall good agreement with the theoretical predictions, except at small muon scattering angles.

**** The 22nd International Workshop on Neutrinos from Accelerators (NuFact2021) ****
**** 6–11 Sep 2021 ****
**** Cagliari, Italy ****

[*] Speaker

PoS(NuFact2021)189

This poster presents the first measurement of exclusive charged-current quasielastic-like (CCQE-like) muon neutrino (ν_μ) differential cross sections on argon (^{40}Ar), measured using the Run 1 data sets from the MicroBooNE liquid argon time projection chamber (LArTPC) [1]. Our results have also been used as a benchmark for theoretical models of ν_μ-^{40}Ar interactions, which are essential in order to perform high precision measurements of the oscillation parameters by future LArTPC experiments.

We focus on interactions that we refer to as CC1p0π, where the contribution of CCQE interactions is enhanced [2]. These interactions include charged-current ν_μ-^{40}Ar scattering events with exactly one detected muon candidate with momentum greater than 100 MeV/c, precisely one proton candidate with momentum greater than 300 MeV/c, any number of neutrons at any momenta, and any number of charged pions with momentum lower than 70 MeV/c. Furthermore, the candidate muon-proton pairs are required to be roughly coplanar with small missing transverse momentum. A minimal residual activity near the interaction vertex that is not associated with the measured muon or proton is also required. For these candidate CC1p0π events, we extract the flux-integrated ν_μ-^{40}Ar differential cross sections as a function of muon and proton momentum and angle. We also report our results in calorimetric measured energy and reconstructed momentum transfer.

The measurement uses data sets from the MicroBooNE LArTPC detector [3], which is the first of a series of LArTPCs to be used for high precision neutrino oscillation measurements [4, 5]. The detector has an active mass of 85 tonnes and is located 463 m downstream from the target. MicroBooNE is also located along the Booster Neutrino Beam (BNB) at Fermilab, which has an energy spectrum up to several GeV that peaks around 0.7 GeV [6].

Muon-proton candidate pairs are identified by requiring two tracks with a common vertex and an energy deposition profile consistent with a proton and a muon [2]. Additional cuts on the track pair opening angle ($35^o < \Delta\theta_{\mu,p} < 145^o$) and the muon and proton track lengths ($l_\mu > l_p$) significantly reduce the cosmic contamination to less than 1%.

To reduce our cosmic background, this selection considers only pairs of tracks with a fully contained proton candidate and a fully or partially contained muon candidate in the fiducial volume of the MicroBooNE detector. The fiducial volume is defined on the ranges 3 < x < 253, -110 < y < 110, and 5 < z < 1031 cm. The z axis points along the direction of the beam, with 0 cm at the upstream edge of the detector. The x axis is along the negative drift direction with 0 cm placed at the anode plane. Finally, the y axis points vertically upward with 0 cm at the center of the detector. Tracks are fully contained if both the start and end points are within this volume. They are partially contained if only the start point is within this volume.

We limit our analysis to a phase-space region where the detector response to our signal is well understood. Namely, we focus on regions where the effective detection efficiency is higher than 2.5%. This limits our results to the ranges $0.1 < p_\mu < 1.5$ GeV/c, $0.3 < p_p < 1.0$ GeV/c, $-0.65 < \cos(\theta_\mu) < 0.95$, and $\cos(\theta_p) > 0.15$. Additional kinematics-based selections are used to enhance the contribution of CCQE interactions in our CC1p0π sample. These include the demand that the candidate muon-proton pairs are on the same ϕ plane ($|\Delta\phi_{\mu,p} - 180^o| < 35^o$) relative to the beam axis, have small missing transverse momentum relative to the beam direction ($p_T = |\vec{p}_\mu + \vec{p}_p| < 350$ MeV/c), and have a small energy deposition around the interaction vertex which is not associated with the muon or proton tracks. After the application of the outlined event selection, we isolated 410 CC1p0π candidate events. Based on the GENIE event generator, we estimate that our CC1p0π

event selection purity equals ≈84%. CCQE interactions account for 81% of the measured events. The efficiency for detecting CC1p0π events within our fiducial volume was estimated using our Monte Carlo (MC) simulation and equals ≈20%. This efficiency includes acceptance effects. The typical LArTPC efficiency for reconstructing a contained high-momentum proton or muon track is greater than ≈90% [7].

Figure 1 illustrates the flux-integrated single differential CC1p0π cross section as a function of the cosine of the reconstructed muon scattering angle. The data points are compared to several event generator predictions and to our GENIE-based MC result used for efficiency corrections and the MC backgrounds in our analysis. The latter is the outcome of analyzing a sample of MC events produced using our "nominal" GENIE model. These MC events are propagated through the full detector simulation in the same way as data.

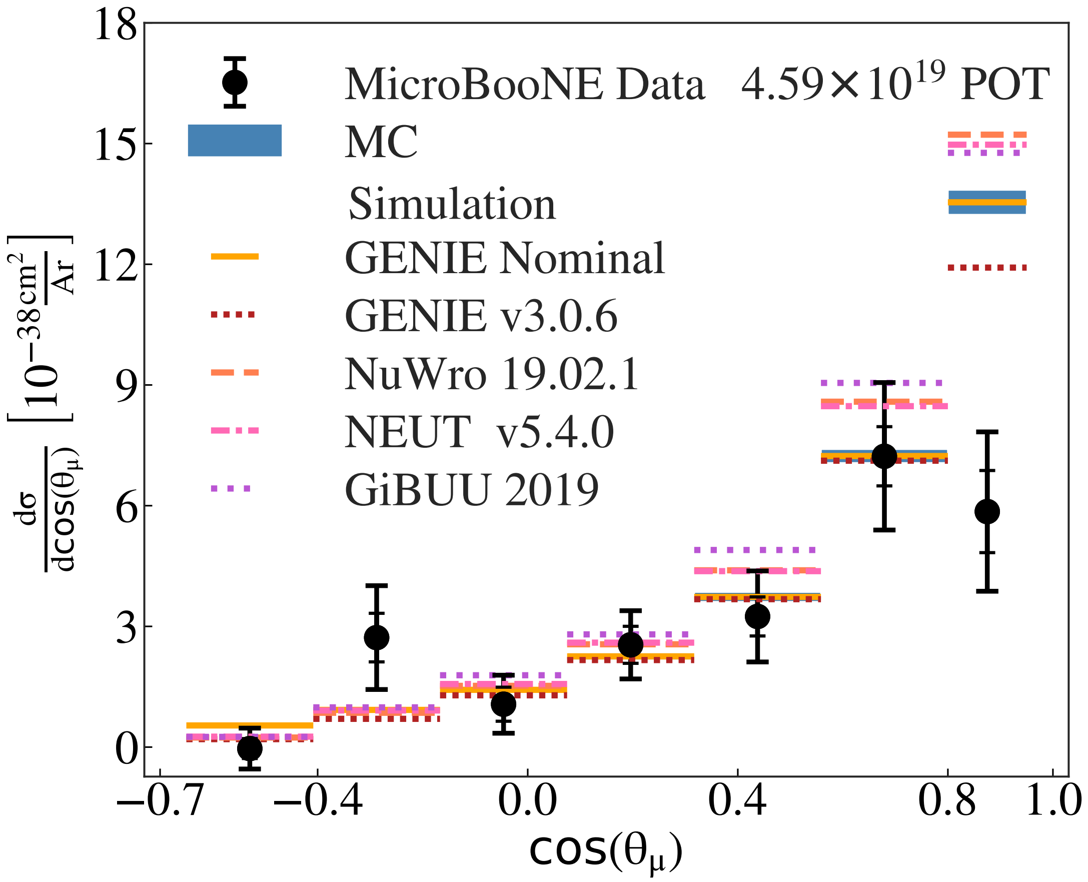

Figure 1: The flux integrated single differential CC1p0π cross sections as a function of the cosine of the measured muon scattering angle. Inner and outer error bars show the statistical and total (statistical and systematic) uncertainty at the 1σ, or 68%, confidence level. Colored lines show the results of theoretical absolute cross section calculations using different event generators (without passing through a detector simulation). The blue band shows the extracted cross section obtained from analyzing MC events propagated through our full detector simulation. The width of the band denotes the simulation statistical uncertainty. Figure adapted from [1].

PoS(NuFact2021)189

This model (GENIE v2.12.2) [8, 9] treats the nucleus as a Bodek-Ritchie Fermi gas, used the Llewellyn-Smith CCQE scattering prescription [11], the empirical MEC model [12], the Rein-Sehgal resonance and coherent scattering model [13], and a data-driven FSI model denoted as "hA" [14].

In addition, theoretical predictions by several other event generators are shown at the cross section level (i.e., with no detector simulations) [15]. These include GENIE v2.12.2 and v3.0.6 [8–10], NuWro 19.02.1 [16], and NEUT v5.4.0 [17]. The agreement between the nominal GENIE calculation (v2.12.2) and the MC prediction constitutes a closure test for our analysis. The other generators all improve on GENIE v2.12.2 by using updated nuclear interaction models. Typical examples would be the use of a local Fermi gas model [18] and random phase approximation corrections [19]. GENIE v3.0.6 and NEUT also include Coulomb corrections for the outgoing muon [20]. The theoretical models implemented in these event generators include free parameters that are typically fit to data, with different generators using different data sets. We also consider the GiBUU 2019 [21] event generator, which fundamentally differs from the others due to its use of a transport equation approach.

As can be seen in Fig. 1, all models are in overall good agreement with our data, except for the highest $\cos(\theta_\mu)$ bin, where the measured cross section is significantly lower than the theoretical predictions. This discrepancy cannot be explained by the systematic uncertainties and is therefore indicative of an issue with the theoretical models. Specifically, high $\cos(\theta_\mu)$ corresponds to low-momentum-transfer events that were previously observed to not be well reproduced by theory in inclusive reactions [22] and is now also seen in exclusive reactions. We note that the high $\cos(\theta_\mu)$ bin has a large contribution from MC beam-related backgrounds, which is estimated using the GENIE-v2.12.2-based MC simulation.

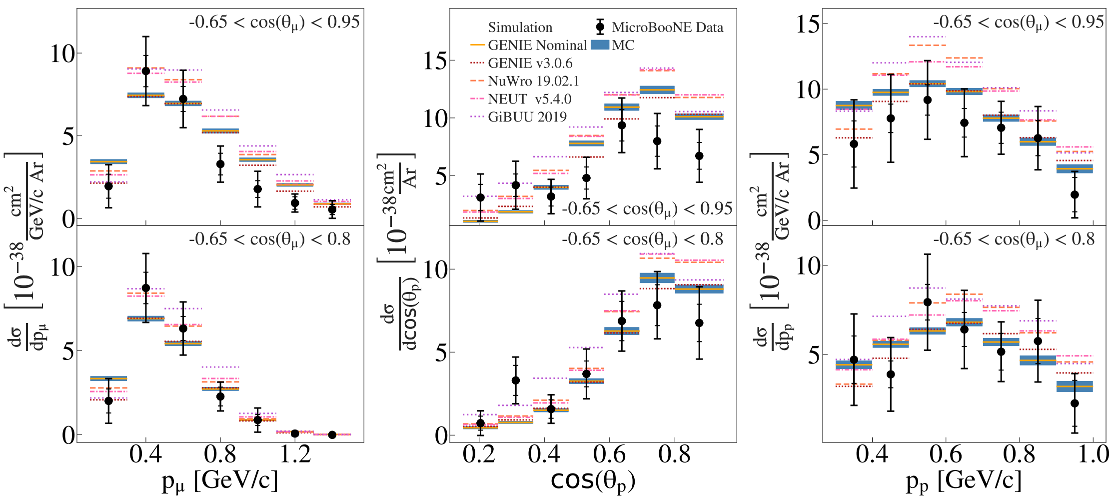

Figure 2: As Fig. 1, but for the differential cross sections as a function of measured muon momentum (left) and measured proton scattering angle (middle) and momentum (right). Cross sections are shown for the full measured phase-space (top) and for events with $\cos(\theta_\mu) < 0.8$ (bottom). Figure adapted from [1].

As the differential cross sections in proton kinematics and muon momentum include contributions from all muon scattering angles, their agreement with the theoretical calculations is affected by this disagreement. Figure 2 shows this comparison between the relevant cross sections in the full

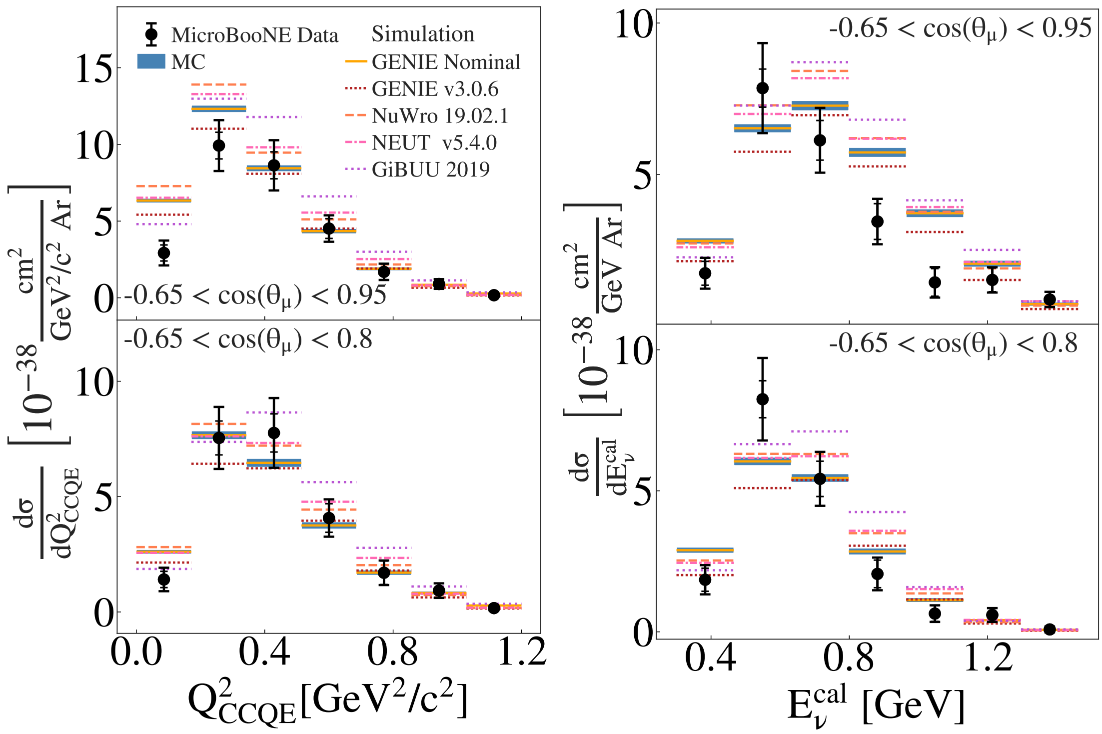

Figure 3: The flux integrated single differential CC1p0π cross sections as a function of $Q^2_{CCQE} = (E^{\text{cal}}_\nu - E_\mu)^2 - (\vec{p}_\nu - \vec{p}_\mu)^2$ and $E^{\text{cal}}_\nu = E_\mu + T_p + BE$, where BE = 40 MeV and $\vec{p}_\nu = (0, 0, E^{\text{cal}}_\nu)$. Inner and outer error bars show the statistical and total (statistical and systematic) uncertainty at the 1σ, or 68%, confidence level. Colored lines show the results of theoretical absolute cross section calculations using different event generators (without passing through a detector simulation). The blue band shows the extracted cross section obtained from analyzing MC events passed through our full detector simulation. Figure adapted from [1].

available phase space (top) and in the case where events with $\cos(\theta_\mu) > 0.8$ are excluded (bottom). Removing this part of the phase space significantly improves the agreement between data and theory.

Figure 3 shows the flux-integrated single differential cross sections as a function of calorimetric measured energy and reconstructed momentum transfer, with and without events with $\cos(\theta_\mu) > 0.8$. The former is defined as $E^{\text{cal}}_\nu = E_\mu + T_p +$ BE and the latter as $Q^2_{CCQE} = (E^{\text{cal}}_\nu - E_\mu)^2 - (\vec{p}_\nu - \vec{p}_\mu)^2$, where E_μ is the muon energy, T_p is the proton kinetic energy, and BE = 40 MeV is the effective nucleon binding energy for ^{40}Ar [23]. E^{cal}_ν is often used as a proxy for the true neutrino energy.

In summary, we report the first measurement of ν_μ-^{40}Ar CCQE-like differential cross sections for event topologies with a single muon and a single proton detected in the final state. The data are in good agreement with theoretical predictions, except at small muon scattering angles that correspond to low-momentum-transfer reactions. This measurement constrains calculations essential for the extraction of oscillation parameters and highlights kinematic regions where improvement of theoretical models is required. The benchmarking of exclusive CC1p0π cross sections on ^{40}Ar presented here suggests that measurements of CC1p0π interactions are a suitable choice for use in precision neutrino oscillation analyses, especially after theoretical models are reconciled with the small scattering angle data.

References

[1] P. Abratenko et al. (MicroBooNE Collaboration), First Measurement of Differential Charged Current Quasielasticlike ν_μ-Argon Scattering Cross Sections with the MicroBooNE Detector, Phys. Rev. Lett. 125, 201803 (2021).

[2] C. Adams et al. (MicroBooNE Collaboration), Rejecting cosmic background for exclusive charged current quasi elastic neutrino interaction studies with Liquid Argon TPCs; a case study with the MicroBooNE detector, Eur. Phys. J. C 79, 673 (2019).

[3] R. Acciarri et al. (MicroBooNE Collaboration), Design and construction of the MicroBooNE detector, JINST 12 P02017 (2017).

[4] M. Antonello et al. (MicroBooNE, LAr1-ND, ICARUS- WA104 Collaborations), A proposal for a three detector short-baseline neutrino oscillation program in the Fermilab booster neutrino beam, arXiv:1503.01520 (2015).

[5] B. Abi et al. (DUNE Collaboration), Deep underground neutrino experiment (DUNE), far detector technical design report, Volume I. Introduction to DUNE, J. Instrum. 15, T08008 (2020).

[6] A. A. Aguilar-Arevalo et al. (MiniBooNE Collaboration), Neutrino flux prediction at MiniBooNE, Phys. Rev. D 79, 072002 (2009).

[7] R. Acciarri et al. (MicroBooNE Collaboration), The Pandora multi-algorithm approach to automated pattern recognition of cosmic-ray muon and neutrino events in the MicroBooNE detector, Eur. Phys. J. C 78, 82 (2018).

[8] C. Andreopoulos et al., The GENIE neutrino Monte Carlo Generator, Nucl. Instrum. Methods Phys. Res., Sect. A 614, 87.(2010).

[9] C. Andreopoulos et al., The GENIE neutrino Monte Carlo generator: Physics and user manual, arXiv:1510.05494 (2015).

[10] L. Alvarez-Ruso et al. Recent highlights from GENIE v3, Eur. Phys. J. Spec. Top. (2021).

[11] C. H. L. Smith, Neutrino reactions at accelerator energies, Phys. Rep. 3, 261 (1972).

[12] T. Katori, Meson exchange current (MEC) models in neutrino interaction generators, AIP Conf. Proc. 1663, 030001 (2015).

[13] D. Rein and L. Sehgal, Neutrino excitation of baryon resonances and single pion production, Ann. Phys. (Leipzig) 133, 79 (1981).

[14] S. G. Mashnik, A J. Sierk, K. K. Gudima, and M. I. Baznat, CEM03 and LAQGSM03: New modeling tools for nuclear applications, J. Phys. Conf. Ser. 41, 340 (2006).

[15] P. Stowell et al., NUISANCE: A neutrino cross-section generator tuning and comparison-framework, J. Instrum. 12, P01016 (2017).

PoS(NuFact2021)189

[16] T. Golan et al., NuWro: The Wroclaw Monte Carlo generator of neutrino interactions, Nucl. Phys. B, Proc. Suppl. 499, 229 (2012).

[17] Y. Hayato, A neutrino interaction simulation program library NEUT, Acta Phys. Polon. B 40, 2477 (2009).

[18] R. C. Carrasco and E. Oset, Interaction of real photons with nuclei from 100-MeV to 500-MeV, Nucl. Phys. A536, 445 (1992).

[19] J. Nieves, J. E. Amaro, and M. Valverde, Inclusive quasielastic charged-current neutrino-nucleus reactions, Phys. Rev. C 70, 055503 (2004).

[20] J. Engel, Approximate treatment of lepton distortion in charged current neutrino scattering from nuclei, Phys. Rev. C 57, 2004 (1998).

[21] U. Mosel, Neutrino event generators: Foundation, status and future, J. Phys. G 46, 113001 (2019).

[22] P. Abratenko et al. (MicroBooNE Collaboration), First Measurement of Inclusive Muon Neutrino Charged Current Differential Cross Sections on Argon at about 0.8 GeV with the MicroBooNE Detector, Phys. Rev. Lett. 123, 131801 (2019).

[23] Bodek, A., Cai, T. Removal energies and final state interaction in lepton nucleus scattering. Eur. Phys. J. C 79, 293 (2019).